Proceedings of the 17th World Congress
The International Federation of Automatic Control
Seoul, Korea, July 6-11, 2008

Control of a Five-Degrees-of-Freedom Nanopositioner

Jing-Chung Shen, *Huan-Keng Chiang, Wen-Yuh Jywe, **Chien-Hung Liu
******Te-Hua Fang,*Yu-Ling Shu, ***Hun-Shu Wang**

Department of Automation Engineering, National Formosa University
Huwei, Yunlin, Taiwan, (Email: jcshen@nfu.edu.tw)
**Department of Electrical Engineering, National Winlin University of Science and Technology*
Douliou, Yunlin, Taiwan
***Institute of Electro-Optical and Material Science, National Formosa University*
Huwei,Yunlin, Taiwan
****Institute of Mechanical Engineering, National Cheng Kung University*
Tainan, Taiwan
*****Institute of Mechanical and Electro-Mechanical Engineering, National Formosa University*
Huwei, Yunlin, Taiwan

Abstract: This paper presents the tracking control of a five-degrees-of-freedom nanopositioner. This nanopositioner is actuated by piezoelectric actuators. Capacitive gap sensors are used for position feedback. Firstly, the modified Prandtl-Ishlinskii (MPI) model is used to model the hysteresis nonlinearity of piezoelectric actuator, and then its inverse is used to cancel out the hysteresis nonlinearity. In order to design the feedback controller, the linearized open-loop characteristics of this nanopositioner are investigated. Based on the results of investigation, each pair of piezoelectric actuator and corresponding gap sensor are treated as independent systems and modeled as a uncertain first order linear model. When the model is identified, the linear system model with uncertainty is used to design the controller. The sliding-mode disturbance (uncertainty) estimation and compensation scheme is used in this study. Experimental results are given to show the effectiveness of the proposed method.

1. INTRODUCTION

Due to the progress in precision engineering, a growing number of motion control applications require sub-micrometer position accuracy. When performing a specific manufacturing or inspection task, often multiple axes must be controlled in coordination. In the literatures (Gao *et al*., 1999, Seugling *et al*., 2002, Shen *et al*., 2007a, Chang *et al*., 1999a, b, Ku *et al*., 2000, Jywe *et al.*, 2004), several multi-degree-of-freedom precision motion stages were reported. Both of these precision motion stages are actuated by piezoelectric actuators.

It is well known that the piezoelectric actuator has many advantages (Ku *et al*., 2000, Cruz-Hernamdez *et al*., 2001) such as: 1) there are no moving parts; 2) the actuators can produce large forces; 3) they have almost unlimited resolution; 4) the efficiency is high; and 5) response is fast. However, it also has some bad characteristics such as: 1) hysteresyis behaviour; 2) drift in time; 3) temperature dependence. Hysteresis characteristics are generally nondifferentiable nonlinearities and usually unknown, this often limits system performance via, e.g., undesirable oscillations or instability. Therefore, it is difficult to obtain an accurate trajectory tracking control.

Recently, several methods have been reported for the trajectory tracking control of a piezoelectric-actuated system. For a survey, please refer the articles (Shen *et al*., 2007a, b).

In this paper, tracking control of a five-degrees-of-freedom nanopositioner is presented. Actuation of this nano-stage is done with piezoelectric actuators. Capacitance-type gap sensors are used for position measurement. Firstly, the structure of this nanopositioner is described. Then, the open-loop system characteristics are experimentally investigated. The modified Prandtl-Ishlinskii (MPI) model (Kuhnen *et al*., 2002, Kuhnen, 2003) is used to model the hysteresis nonlinearity of piezoelectric actuator and then its inverse is used to cancel out the hysteresis nonlinearity. Base on the results of investigation, each pair of piezoelectric actuator and corresponding gap sensor are treated as independent systems and modelled as an uncertain first order linear model. In this study, the sliding-mode uncertainty (disturbance) estimation and compensation scheme (Utkin *et al*., 1999, Shen, 2002, Shen *et al*., 2007a, b) is used to compensate the uncertain system. Finally, the experimental results are presented.

2. THE NANOPOSITIONER AND EXPERIMENTAL SETUP

The structure of the nanopositioner is shown in Fig. 1. This nanopositioner is a flexure hinge-based stack-type design and can provide heavy payload (more than 2 kilogram) (Jywe *et al*., 2004). All the parts are out of medium carbon steel. It is composed of six piezoelectric actuators, six preload adjusting mechanisms, a rigid base, eight rotational flexure hinges; a four-side flexure hinges fixture and six capacitance-type gap sensors. The actuators were fastened at each end to the rigid base using the preload adjusting

mechanisms. These actuators are set up to provide the translational motion of the X-axis (X), Y-axis (Y), Z-axis (Z) and the uniformly rotational motion along the X-axis (θ_x) and Y-axis (θ_y). Gap sensors are placed to measure the displacement of each sides of the stage platform and the displacements of X and Y directions. Moreover, six micrometers are provided to adjust the mechanical zero point of the gap sensors.

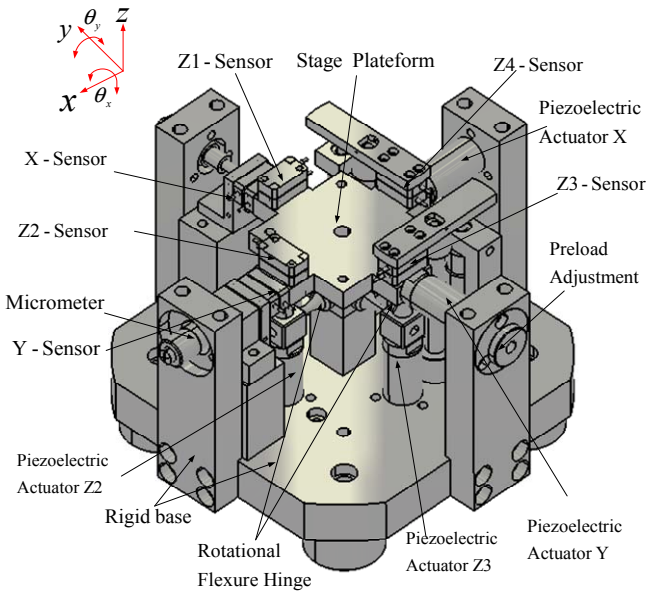

Fig. 1. The structure of the nanopositioner.

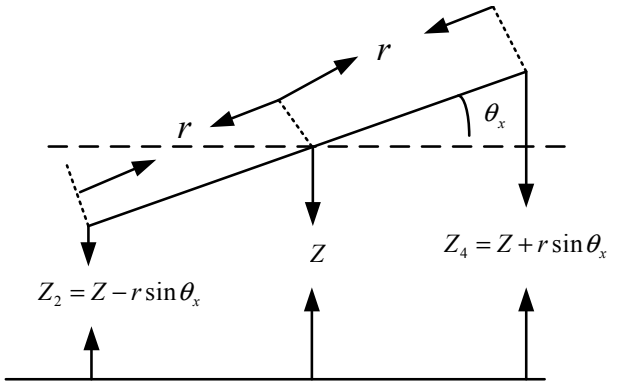

Fig. 2. The relation between Z_2 , Z_4 and Z , θ_x .

Base on the geometric relation (refer to Fig. 2), the relations between Z_2 (The displacement measured by sensor Z_2), Z_4 and Z (The displacement of the centre of the stage platform in Z-axis), θ_x can be obtained as $Z_2 = Z - r\sin\theta_x$ and $Z_4 = Z + r\sin\theta_x$ respectively. Where r (25.5mm) is the half of the distance between the centre of sensors Z_2 and Z_2. Note that θ_x is small (inside ±60 second), therefore, $\sin\theta_x \approx \theta_x$. Similarly, the relations between Z_1 , Z_3 and Z, θ_y can be obtained. The relations between Z_1 , Z_2 , Z_3 , Z_4 and Z, θ_x , θ_y can be summarized as

$$\begin{bmatrix} Z_1 \\ Z_2 \\ Z_3 \\ Z_4 \end{bmatrix} = \begin{bmatrix} 1 & 0 & r \\ 1 & -r & 0 \\ 1 & 0 & -r \\ 1 & r & 0 \end{bmatrix} \begin{bmatrix} Z \\ \theta_x \\ \theta_y \end{bmatrix} \quad (1)$$

The piezoelectric actuators (PSt150/7/20 Vs12) that we used are manufactured by Piezomechanik GmbH with nominal expansion 20 μm (at 150V). The range of input voltage to the piezoelectric actuators is from 0 to 150V. The gap sensors (D-015) are also from Piezomechanik GmbH. The measured range of the gap sensors are extended by a factor of three. Therefore, total ranges of the gap sensors are 45 μm with a sensitivity of 0.222 $V / \mu m$. There are six piezoelectric actuators and six gap sensors, thus the whole control system have six inputs and six outputs. Control of this nanopositioner is done with a controller board with a Power PC central processing unit (DS1103, dSPACE GmbH). The sampling rate of the control algorithm was 10 KHz. The resolution of A/D converters is 16-bit.

3. OPEN-LOOP CHARACTERISTICS OF THE NANOPOSITIONER

In order to design the controller properly, it is necessary to understand the open-loop characteristics of this nanopositioner. Firstly, the maximum moving range and hysteresis nonlinearity of piezoelectric actuators are investigated by static tests. A low frequency (0.5Hz) triangle wave is used to drive the piezoelectric actuators respectively and the displacements measured by sensors are recorded. From the results, it is found that the moving ranges of X, Y, Z_1 , Z_2 , Z_3 and Z_4 are about 13.6 μm , 11.5 μm , 15 μm , 16 μm , 14.5 μm and 14.5 μm respectively. Moreover, the coupling effects between X, Y, Z_1 , Z_2 , Z_3 and Z_4 are less than 18%.

The frequency-response experiments also are conducted. When measuring the frequency response, a bias voltage was added to one actuator to push one side of the stage platform to the centre of the moving range. Then, a random excitation signal was sent to this piezoelectric actuator and the displacements are measured by the gap sensor. In order to reduce the effect of hysteresis nonlinearity, the amplitude of the excitation signal is kept small. Fig. 3 shows the test results obtained by driving actuator X. As seen in Fig.3, the coupling effects are less than 18% in magnitude. This coincides with the results of static test. A linear dynamic model, represented as a transfer function in the Laplace domain, relating the input voltage of actuator X, to the output of sensor X, was estimated. The poles of this model are {-430, -7600 ± j31400}. It is found that the slowest pole is -430 and the others poles are more than ten times faster this pole. Therefore, it is possible to model the sub-system by a first-order transfer function.

4. SYSTEM MODELING AND CONTROLLER DESIGN

In this section, hysteresis model, system dynamic model and controller design for the nanopositioner are presented. For

simplicity, the whole control system was divided into six single-input-single-output sub-systems. Each sub-system consisted of a piezoelectric actuator and its corresponding gap sensor. Then, the controllers were designed for each sub-system independently and regarded the coupling effects between each sub-system as disturbances.

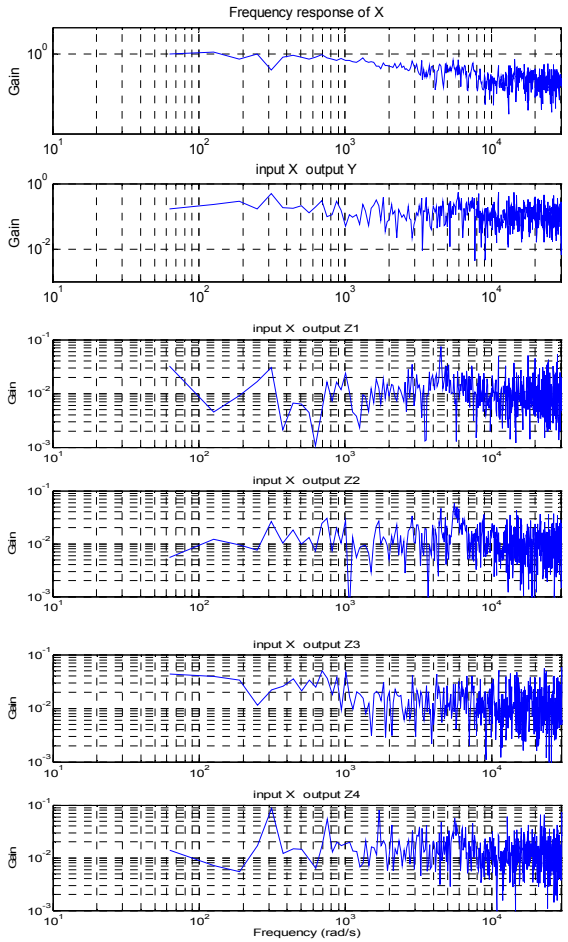

Fig. 3. Frequency response of the nanopositioner (By driving actuator X.).

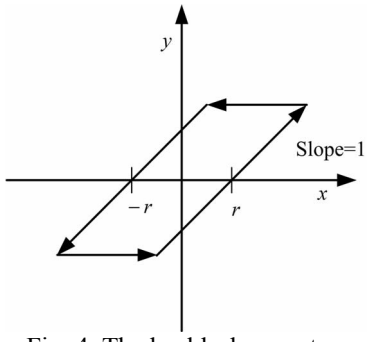

Fig. 4. The backlash operator.

4.1 Modified Prandtl-Ishlinskii hysteresis model

There are two elementary operators in the MPI hysteresis model. One is the backlash operator (see Fig. 4) that is defined by

$$y(kT_s) = H_r[x(kT_s), y_0] \tag{2}$$

$$H_r[x(kT_s), y_0] = \max\{x(kT_s) - r, \min\{x(kT_s) + r, y((k-1)T_s)\}\} \tag{3}$$

where x is the control input, T_s is the sampling interval, k indicates the sampling point ($1 \le k \le n_s$, n_s is the quantity of sampled data), y is the output of the operator, and r is the magnitude of the backlash. The initial condition of (2) is given by

$$y(0) = \max\{x(0) - r, \min\{x(0) + r, y_0\}\} \tag{4}$$

where the initial state $y_0 \in R$, and is usually but not necessarily initialized to 0. The other operator is the one-sided dead-zone operator (see Fig. 5) that is defined by

$$S_d[x] = \begin{cases} \max\{x - d, 0\} & \text{for } d > 0 \\ x & \text{for } d = 0 \\ \min\{x - d, 0\} & \text{for } d < 0 \end{cases} \tag{5}$$

where $d \in R$ is the threshold of the operator.

Hysteretic nonlinearities can be modelled by a linearly-weighted superposition of many backlash operators with different magnitudes and weight values in series with a linearly-weighted superposition of many one-sided dead-zone operators with different thresholds and weight values given by

$$\mathrm{H}[x(kT_s)] = \sum_{j=-m}^{m} w_{sj} S_{d_j}\left[\sum_{i=0}^{n} w_{hi} H_{r_i}[x(kT_s), y_{0i}]\right] \tag{6}$$

where w_{hi} and w_{sj} are the weightings of the backlash operators and dead-zone operators, r_i are the magnitude of backlashes sorted so that $0 = r_0 < r_1 < \ldots < r_n$, d_j are the threshold values sorted so that

$$d_{-m} < \ldots < d_{-1} < d_0 = 0 < d_1 < \ldots < d_m,$$

and y_{0i} are the initial states. The values of r_i and d_j are usually chosen to be equally spaced in the admissible value ranges.

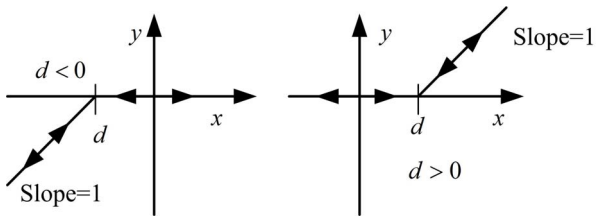

Fig. 5. The one-sided dead-zone operator.

4.2 Inverse model of hysteretic nonlinearities

When the weights of the backlash operators and dead-zone operators satisfy some constraints, the inverse model of $\mathrm{H}[x]$ exists and is given by (Kuhnen, 2003)

$$\mathrm{H}^{-1}[y(kT_s)] = \sum_{i=0}^{n} w'_{hi} H_{r'_i}\left[\sum_{j=-m}^{m} w'_{sj} S_{d'_j}[y(kT_s)], z_{0i}\right] \tag{7}$$

The parameters of the inverse model can be found by

$$w'_{h0} = 1/w_{h0}, \tag{8}$$

$$w'_{hi} = -\frac{w_{hi}}{(w_{h0} + \sum_{l=1}^{i} w_{hl})(w_{h0} + \sum_{l=1}^{i-1} w_{hl})}, \text{ for } i = 1, 2, .., n \quad (9)$$

$$z_{0i} = \sum_{l=0}^{i} w_{hl} y_{0i} + \sum_{l=i+1}^{n} w_{hl} y_{0l}, \text{ for } i = 0, 1, 2, .., n \quad (10)$$

$$r'_i = \sum_{l=0}^{i} w_{hl}(r_i - r_l); \text{ for } i = 0, \ldots, n, \quad (11)$$

$$w'_{s0} = 1 / w_{s0}, \quad (12)$$

$$w'_{sj} = -\frac{w_{sj}}{(w_{s0} + \sum_{l=1}^{j} w_{sl})(w_{s0} + \sum_{l=1}^{j-1} w_{sl})}, \text{ for } j = 1, \ldots, m, \quad (13)$$

$$w'_{sj} = -\frac{w_{sj}}{(w_{s0} + \sum_{l=j}^{-1} w_{sl})(w_{s0} + \sum_{l=j+1}^{-1} w_{sl})}, \text{ for } j = -m, \ldots, -1, \quad (14)$$

$$d'_0 = 0, \quad (15)$$

$$d'_j = \sum_{l=0}^{j} w_{sl}(d_j - d_l), \text{ for } j = 1, \ldots, m, \quad (16)$$

and

$$d'_j = \sum_{l=j}^{0} w_{sl}(d_j - d_l), \text{ for } j = -m, \ldots, -1. \quad (17)$$

Fig. 6 shows the hysteresis nonlinearity and its MPI model ($n = 15$, $m = 4$) of actuator Z_2. It can be seen that the model can match the hysteresis nonlinearity very well.

4.3 System Dynamic Model

Based on the test results described in last section, each sub-system can be modelled by a first order uncertain linear system as shown in Fig. 7. Where u is the input of the inverse hysteresis model, H is the hysteresis nonlinearity of the piezoelectric actuator, d represents the disturbance and the first order differential equation

$$T(1 + \Delta(t))\dot{x} + x = v, \quad (18)$$

describes the dynamic behaviour of the sub-system. Where x is the displacement, T is the nominal time constant and $\Delta(t)$ represents the uncertainty. Parameter T and the bound of $\Delta(t)$ can be determined by doing step response tests at various working points.

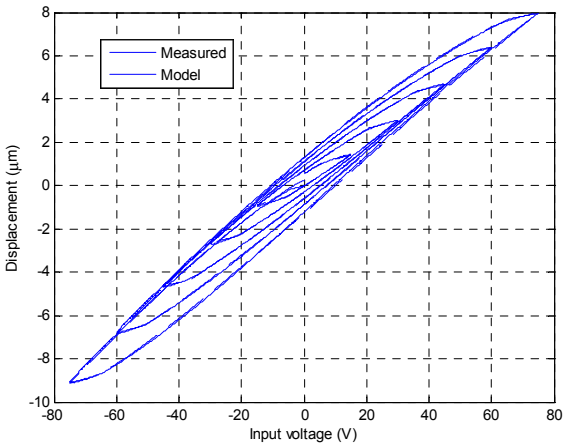

Fig. 6. Hysteresis nonlinearity and its MPI model of actuator Z_2.

From Fig. 7, v can be represented as

$$v = \mathrm{Ku} + N(t) + d(t), \quad (19)$$

where K is the linearized gain (Equal to 1 after the inverse model compensation.) and $N(t)$ represents the remained nonlinear uncertain part of the hysteresis. From (18) and (19), the following dynamic equation can be obtained:

$$\dot{x} = -\frac{x}{T} + \frac{Ku}{T} + \phi(t) \quad (20)$$

where

$$\phi(t) = \frac{\Delta(x - Ku) + N + d}{T(1 + \Delta)}$$

represents the disturbance and uncertainties.

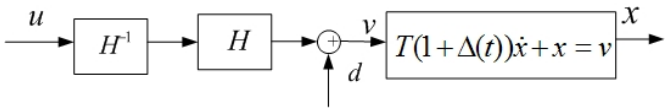

Fig. 7. Model of the sub-system.

4.4 Sliding-mode Controller Design

This subsection describes how to design the sliding mode controller. In this study, the sliding mode disturbance (uncertainty) estimation and compensation scheme is applied to design the closed-loop controller for the sub-system.

Let x_d be the desired displacement, which may be time varying. Define

$$e = x_d - x \quad (21)$$

as the tracking error. From (19) and (20), the error dynamics can be obtained as

$$\dot{e} = \dot{x}_d - \dot{x} = \dot{x}_d + \frac{x}{T} - \frac{K}{T}u - \phi(t). \quad (22)$$

Let the control law be

$$u = \frac{x}{K} + \frac{T}{K}(\lambda e + \dot{x}_d) + u_d \quad (23)$$

where λ is the feedback gain to be designed so that the error dynamic will have the desired response while the system is free of disturbance and uncertainty, and u_d is the uncertainty and the disturbance compensation component yet to be determined by the sliding mode estimator.

Defining the switching function as

$$S = z - e \tag{24}$$

with

$$\dot{z} = -\lambda e - \frac{K}{T} u_d + \psi, \quad z(0) = e(0) \tag{25}$$

where z is the state variable of this auxiliary process, ψ is the switching action assigned as

$$\psi = -\eta \text{sign}(S), \quad \text{sign}(S) = \begin{Bmatrix} 1 & for & S > 0 \\ -1 & for & S < 0 \end{Bmatrix} \tag{26}$$

and the positive constant η satisfies

$$\eta > |\phi(t)| \tag{27}$$

Ensuring a sliding regime $S = 0$ requires consideration of the Lyapunov candidate $V = 0.5S^2$. Differentiating V with respect to time and substituting (22-25) to obtain

$$\dot{V} = S(\dot{z} - \dot{e}) = S[(-\eta \text{sign}(S) + \phi(t))] \tag{28}$$

From (27) and (28), it is seen that

$$\dot{V} < 0 \qquad \text{if} \quad S \neq 0 \tag{29}$$

Thus the sliding condition is satisfied. Note that $z(0) = e(0)$, therefore

$$S = 0 \quad \text{for} \quad t = 0 \tag{30}$$

From (29) and (30), it can be concluded that the sliding mode exists at all times, *i.e.*,

$$\dot{S} = 0 \quad \text{for all} \ t \geq 0 \tag{31}$$

Denote the equivalent value of ψ as ψ_{eq}. Since $\dot{S} = 0$, ψ_{eq} can be determined from (22), (24) and (25):

$$\psi_{eq} = -\phi \tag{32}$$

This means that the equivalent value of ψ equals the uncertainties and disturbances. By selecting $u_d = T\psi_{eq} / K$, the uncertainties and disturbances can be compensated. It was shown in (Utkin *et al.*, 1999) that the equivalent ψ_{eq} is equal to the average value measured by a first-order linear filter with the switched action as its input. Therefore, u_d can be written as

$$u_d = \frac{T}{K}\psi_{av} = \frac{T}{K}\psi_{eq} \tag{33}$$

with

$$\tau\dot{\psi}_{av} + \psi_{av} = \psi . \tag{34}$$

The time constant τ should be made small enough that the plant and disturbance dynamics are allowed to pass through the filter without significant phase delay. Substituting (34) and (23) into (22) yields

$$\dot{e} + \lambda e = -\psi_{eq} - \phi ,$$

which is equivalent to $\dot{e} + \lambda e = 0$. This equation represents the desired error dynamics. This controller is almost as simple as PID controller.

When designing the controllers, the nominal time constant T and the bound of uncertainty Δ can be obtained by step response tests. It was found that the nominal time constants of sub-systems X, Y, Z_1, Z_2, Z_3 and Z_4 are 3.5ms, 3ms, 3ms, 3.5ms, 3.5ms and 4ms respectively. In order to obtain wider bandwidth, λ for each sub-system are chosen as large as possible. Finally, the controller parameters for all sub-system are chosen to be the same as $\lambda = 550$, $\eta = 15$ and $\tau = 0.0036$.

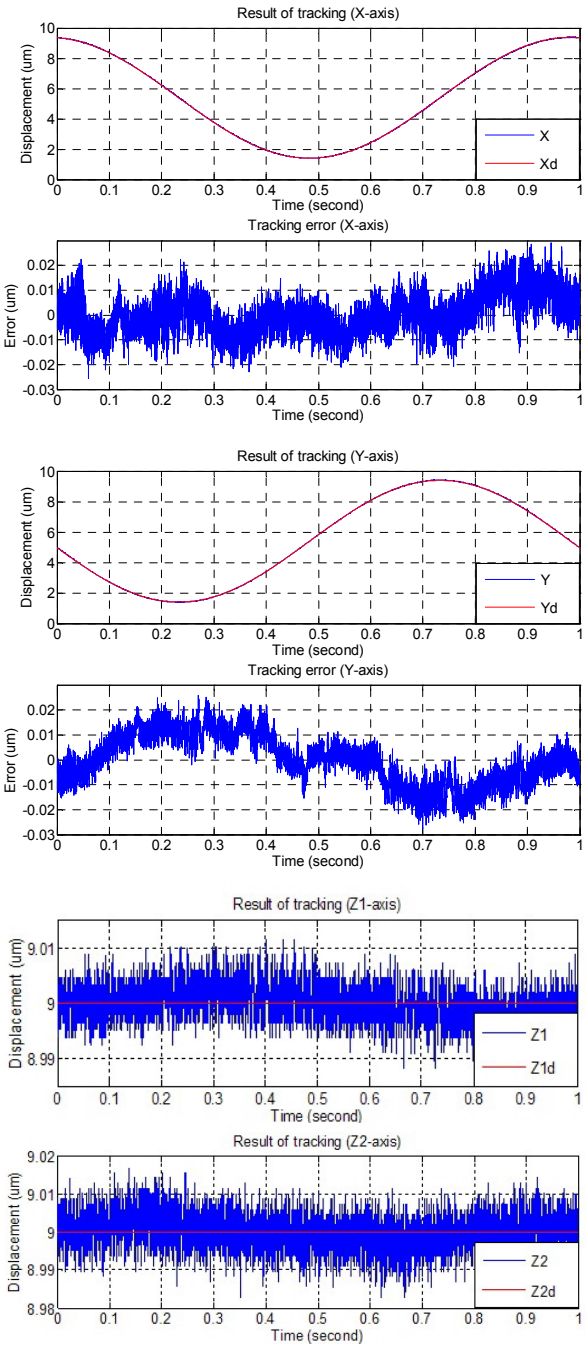

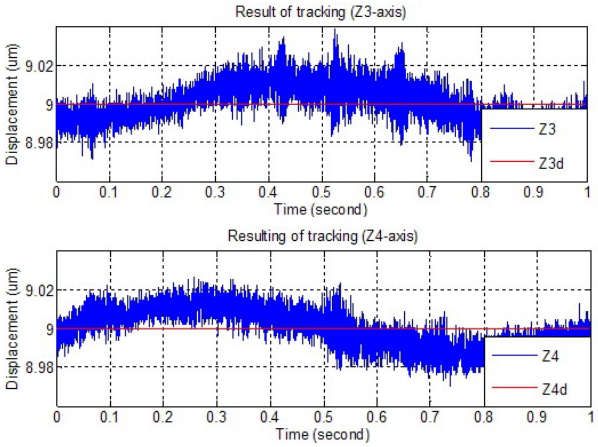

Fig. 7. Control results of tracking a circle on X-Y plane.

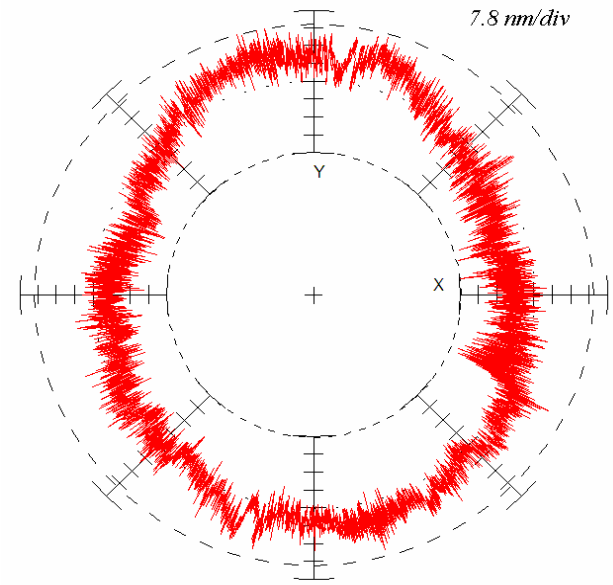

Fig. 8. Result of error analysis.

5. CONTROL RESULTS AND FUTURE WORKS

In order to evaluate the performance of the controller, some experiments were conducted. Due to limited space, only one experimental result is shown here. Fig. 7 depicts the control results of tracking a circle with diameter 8 μm in X-Y plane, $\theta_x = 0$, $\theta_y = 0$ and Z fixed at 9 μm. Fig. 8 shows the result of error analysis. It can be seen that the maximum deviation is about 0.0312 μm (0.78%). The errors in positions Z_1 and Z_2 are inside $\pm 15nm$ while the errors in positions Z_3 and Z_4 are inside $\pm 40nm$. The errors in positions Z_3 and Z_4 are larger than those in positions Z_1 and Z_2. The reason is that the actuators of X-axis and Y-axis act in positions Z_3 and Z_4. This makes the coupling effects obvious.

In this study, the whole control system was divided into six single input single output subsystems and treated the coupling effects as disturbances. In the future, we will take the coupling effects between X, Y, Z_3 and Z_4 into consideration to improve the performance of tracking control.

REFERENCES

Chang, S. H., C. K. Tseng and H. C. Chien (1999a). An ultra-precision XY θ_z piezo-micropositioner part I: design and analysis. *IEEE Trans. On Ultrasonics, Ferroelectrics, and Frequency Control*, **46**, 897-905.

Chang, S. H., C. K. Tseng and H. C. Chien (1999b). An ultra-precision XY θ_z piezo-micropositioner part II: experiment and performance. *IEEE Trans. On Ultrasonics, Ferroelectrics, and Frequency Control*, **46**, 906-912.

Cruz-Hernandez, J. and V. Hayward (2001). Phase Control Approach to Hysteresis Reduction. *IEEE Transaction on Control Systems Technology*, **9**, 17-26.

Gao, P. and S. M., Swei (1999). A six-degree-of-freedom micro-manipulator based on piezoelectric translators. *Nanotechnology*, **10**, 447-452.

Jywe, W. Y., J. C., Shen, Y. F., Teng, C. H. Liu and Y. T., Jian (2004). Development of a flexure hinge based stack-type five-degree-of-freedom nanometer positioning stage. *Journal of Chinese Institute of Mechanical Engineering,* **25**, 465-474.

Ku, S. S., U. Pinsopon, S. Cetinkunt and S. Nakajima (2000). Design, Fabrication, and Real-Time Neural Network Control of a Three-Degrees-of-Freedom Nanopositioner. *IEEE/ASME Transactions on Mechatronics*, **5**, 273-280.

Kuhnen, K. (2003). Modeling, identification and compensation of complex hysteretic nonlinearities: a modified Prandtl-Ishlinskii approach. *European Journal of Control*, **9**, 407-417.

Kuhnen, K. and Janocha H. (2002). Complex hysteresis modeling of a broad class of hysteretic actuator nonlinearities. *Proceedings of the 8th international conference on new actuators*. 688-691.

Seugling, R. M., T. LeBrun, S. T. Smith and L. P. Howard (2002). A six-degree-of-freedom precision motion stage. *Review of Scientific Instruments*, **73**, 2462-2468.

Shen, J. C. (2002). H^∞ Control and Sliding Mode Control of Magnetic Levitation System. *Asian Journal of Control*, **4**, 333-340.

Shen, J. C., W. Y. Jywe, C. H. Liu, Y. T. Jian and J. Yang (2007a). Sliding-mode Control of a Three-Degrees-of-Freedom Nanopositioner. *Asian Journal of Control*. To appear.

Shen, J. C., W. Y. Jywe, H. K. Chiang and Y. L. Shu (2007b). Precision Tracking Control of a Piezoelectric-actuated System. *Precision Engineering*, doi:10.1016/ j.precisioneng.2007.04.002.

Utkin V., J. Guldner and J. Shi (1999). *Sliding Mode Control in Electromechanical Systems*, Taylor & Francis, Padstow.